Effect of the 2022 summer drought across forest types in Europe

Mana Gharun[1], Ankit Shekhar[2,3], Jingfeng Xiao[4], Xing Li[5], Nina Buchmann[2]

[1] Institute of Landscape Ecology, University of Münster, Münster, Germany
[2] Institute of Agricultural Sciences, ETH Zürich, Zürich, Switzerland
[3] Agricultural and Food Engineering Department, Indian Institute of Technology Kharagpur, Kharagpur, India
[4] Earth Systems Research Center, University of New Hampshire, New Hampshire, USA
[5] Research Institute of Agriculture and Life Sciences, Seoul National University, Seoul, South Korea

Correspondence to: Mana Gharun, mana.gharun@uni-muenster.de

Abstract

Forests in Europe experienced record-breaking dry conditions during the 2022 summer. The direction in which various forest types respond to climate extremes during their growing season is contingent upon an array of internal and external factors. These factors include the extent and severity of the extreme conditions and the tree ecophysiological characteristics adapted to environmental cues, which exhibit significant regional variations. In this study we aimed to: 1) quantify the extent and severity of the extreme soil and atmospheric dryness in 2022 in comparison to two most extreme years in the past (2003 and 2018), 2) quantify response of different forest types to atmospheric and soil dryness in terms of canopy browning and photosynthesis, and 3) relate the functional characteristics of the forests to the emerging responses observed remotely at the canopy level. For this purpose, we used spatial meteorological datasets between 1970 to 2022 to identify conditions with extreme soil and atmospheric dryness. We used the near-infrared reflectance of vegetation (NIRv) derived from the MOderate Resolution Imaging Spectroradiometer (MODIS), and the OCO-2 solar induced fluorescence (GOSIF) as an observational proxy for ecosystem gross productivity, to quantify the response of forests at the canopy level.

Deleted: 3
Deleted: 4
Formatted: Superscript
Formatted: Superscript
Formatted: Font colour: Text 1
Deleted: Universitätstrasse 2, 8092
Formatted: Font colour: Text 1
Formatted: Font colour: Text 1
Formatted: Font colour: Text 1
Formatted: Font colour: Text 1
Deleted: 721302
Formatted: Font colour: Text 1, Superscript
Formatted: Font colour: Text 1
Formatted: Font colour: Text 1
Deleted: 3
Deleted: 4

In summer 2022, southern regions of Europe experienced exceptionally pronounced atmospheric and soil dryness. These extreme conditions resulted in a 30% more widespread decline in GOSIF across forests compared to the drought of 2018, and 60% more widespread decline compared to the drought of 2003. Although the atmospheric and soil drought were more extensive and severe (indicated by a larger observed maximum z-score) in 2018 compared to 2022, the negative impact on forests, as indicated by declined GOSIF, was significantly larger in 2022. Different forest types were affected in varying degrees by the extreme conditions in 2022. Deciduous broad-leaved forests were the most negatively impacted due to the extent and severity of the drought within their distribution range. In contrast, areas dominated by Evergreen Needle-Leaf Forests (ENF) in northern Europe experienced a positive soil moisture (SM) anomaly and minimal negative vapor pressure deficit (VPD) in 2022. These conditions led to enhanced canopy greening and stronger solar-induced fluorescence (SIF) signals, benefiting from the warming. The higher degree of canopy damage in 2022, despite less extreme conditions, highlights the evident vulnerability of European forests to future droughts.

Keywords: *photosynthesis, soil drought, atmospheric drought, canopy browning, gross primary production*

Introduction

The frequency and intensity of drought events have been rising globally, and future global warming is expected to further increase their occurrence (Seneviratne et al. 2012; Röthlisberger and Papritz 2023). Particularly over the past two decades, many regions in Europe have experienced widespread drought conditions, notably during the summers of 2003, 2010, and 2018 (Bastos et al. 2020; Zhou et al. 2023). The extreme conditions caused widespread ecological disturbances (Müller and Bahn 2022) and reduced the capacity of forests for carbon uptake, thereby diminishing their potential for mitigating climate change (van der Woude et al. 2023). Additionally, heatwaves and prolonged droughts stress vegetation, making it more susceptible to other biotic and abiotic stress factors. This increased vulnerability leads to higher tree mortality, elevated wildfire risks,

Deleted: Forests in Europe experienced record-breaking dry conditions during the 2022 summer. The direction in which various forest types respond to climate extremes during their growing season is contingent upon an array of internal and external factors. These factors include the extent and severity of the extreme conditions and the tree ecophysiological characteristics adapted to environmental cues, which exhibit significant regional variations. In this study we aimed to: 1) quantify the extent and severity of the extreme soil and atmospheric dryness in 2022 in comparison to two most extreme years in the past (i.e., 2003, 2018), 2) quantify response of different forest types to atmospheric and soil drought in terms of canopy browning and photosynthesis, and 3) relate the functional characteristics of the forests to the emerging responses observed at the canopy level. For this purpose, we used the ERA5-Land spatial meteorological dataset between 1970 to 2022 to identify conditions with extreme soil and atmospheric dryness. We used the near-infrared reflectance of vegetation (NIRv) derived from the MOderate Resolution Imaging Spectroradiometer (MODIS), and the OCO-2 solar induced fluorescence (SIF) as an observational proxy for photosynthesis based on the SIF data product, to quantify the response of forests at the canopy level.¶ In summer 2022, particularly southern regions of Europe experienced the most pronounced atmospheric and soil dryness. As a result, the extremely dry conditions led to an average 30% more widespread decline in SIF across forests compared to drought in 2018, and 60% more widespread decline compared to drought in 2003. Although the atmospheric and soil drought were more extensive and severe (indicated by a larger observed max z-score) in 2018 compared to 2022, the negative impact on forests, indicated by declined SIF, was significantly larger in 2022. Across different forest types, the deciduous broad-leaved forests were most negatively affected by the extrer ... [1]

Deleted: Higher degree of canopy damage in 2022 in spite of less extreme conditions compared to the previous extreme year points to a legacy effect on forest canopies, and a declined forest resilience in response to more frequent drought events.

Deleted: ¶

Deleted: The frequency and intensity of drought events have been increasing globally, and future global warming will continue to increase the occurrence of such events …

Deleted: over

Deleted: , there have been reports of widespread drought conditions, for example during the summers of 2003, 2010 and 2018…

Deleted: Such

Deleted: lead to

Deleted: which

Deleted: es

and a loss of biodiversity among plants and animals living at the edge of their temperature tolerance. These conditions also alter phenology and plant development, causing cascading effects on ecosystem functioning (Seidl et al. 2017).

The spatial extent and severity of drought events vary, and their impacts depend on local ecological characteristics of the forests, species-specific temperature and moisture thresholds that limit tree functioning, as well as adaptation strategies and acclimation of trees to more frequent and intense extreme conditions (Gessler et al. 2020). For example, comparing the 2003 and 2018 extreme years, the year 2018 was characterized by a climatic dipole, featuring extremely hot and dry weather conditions north of the Alps but comparably cool and moist conditions across large parts of the Mediterranean. Negative drought impacts appeared to affect an area 1.5 times larger and to be significantly stronger in summer 2018 compared to summer 2003 (Buras et al. 2020).

In 2022, Europe faced its second hottest and driest year on record, with the summer of that year being the warmest summer ever recorded. Conditions in summer 2022 led to record-breaking heatwave and drought events across many regions (Copernicus Climate Change Service, 2023). Compound drought and heatwave conditions in 2022 caused widespread crop damage, water shortages, and wildfires across Europe. The hardest-hit areas were the Iberian Peninsula, France, and Italy, where temperatures exceeded 2.5°C above normal, and severe droughts persisted from May to August (Tripathy and Mishra 2023). The reduced soil moisture due to precipitation deficits and high temperatures, contributed to the persistence and severity of drought, creating a positive feedback loop where dry soils led to even drier conditions (Tripathy and Mishra 2023).

Drought and heatwaves have a range of detrimental effects on trees and forests. The most immediate impact is that elevated air temperatures and increased dryness, whether in the soil or in the atmosphere, disrupt mesophyll and stomatal conductance, thereby impairing carbon uptake (Marchin et al. 2021). Plants reduce stomatal conductance under severe drought to reduce water stress at the expense of reduced rates of photosynthesis (Oren et al., 1999). Drought also increases the chance of hydraulic failure, which can lead to tree mortality (Choat et al. 2018). Additionally, rising temperatures reduce the enzymatic activity in trees, which in turn diminishes the forest´s gross primary productivity (Gourlez de la Motte et al. 2020). Elevated temperatures can also increase respiration

Deleted: Additionally, heatwave and prolonged drought periods stress vegetation and increase their susceptibility to other biotic and abiotic stress factors, increase tree mortality and risk of wildfire, lead to loss of biodiversity of plants and animals that live on the edge of their temperature tolerance, and change phenology and plant development with cascading effects on the functioning of the ecosystem

Deleted: the

Deleted: and

Deleted: more

Deleted: experienced

Deleted: and

Deleted: 2022

Deleted: was

Deleted: diverse negative

Deleted: impacts

Deleted: the functioning of

Deleted: response

Deleted: rising

Deleted: (

Deleted:)

Deleted: leads to changes in

Deleted: that affect

Deleted: and leads

Deleted: In addition, under

Deleted: of

Deleted: is reduced which also decreases

Deleted: of the forest

Deleted: rates of

rates in both soil and trees, which reduces the forest´s net carbon uptake and their ability to mitigate anthropogenic CO_2 emissions (van der Molen et al. 2011; Anjileli et al. 2021). Drought also restricts the movement of nutrients in soil water, reducing their availability to trees and consequently impacting their growth and productivity (Bauke et al. 2022). Changes in plant water-use and nutrient cycling can trigger feedback loops that magnify the effects of drought and heat stress. For instance, reduced plant cover can increase soil temperatures and further accelerate water loss and increase plant water demand (Haesen et al. 2023). On the other hand, increased atmospheric dryness or reduced soil moisture levels increase stomatal closure which limits transpiration and leads to higher leaf temperature that intensifies heat stress on plants (Drake et al. 2018). Reduced transpiration and photosynthesis elevate surface temperatures and atmospheric CO_2 concentrations, altering local and regional climate patterns and intensifying the frequency and severity of extreme events (Humphrey et al. 2018). These effects vary significantly depending on forest type and species composition. Together with the characteristics of the extreme events themselves – such as their extent and severity- this variability complicates our understanding of how drought affects the functionality of different forest ecosystems (Gharun et al. 2020; Shekhar et al. 2023a). These feedback loops highlight the urgent need to assess how climate extremes impact different forest types, which are crucial for sequestering significant portions of anthropogenic emissions. Our study aims to 1) quantify the extent and severity of the extreme conditions in 2022 – focusing on soil and atmospheric dryness-, and compare them to those of two previous extreme years (2003, 2018), 2) quantify the responses of different forest types to drought in terms of canopy browning and photosynthesis, and 3) connect the functional characteristics of the forests with the canopy-level responses observed.

Methods

Meteorological dataset

We used Europe-wide gridded datasets covering daily mean air temperature (Tair; °C), daily mean relative humidity (RH; %) and daily mean soil moisture (SM; m^3m^{-3}) for the topsoil layer (0-7 cm depth), spanning from 2000-2022. The study area encompasses

Deleted: from the…n both soil and from the …rees, which leads to …educes the forest´sd…net capacity of forests for …arbon uptake and their ability reducing…o mitigate anthropogenic CO_2 emissions (van der Molen et al. 2011; Anjileli et al. 2021). Drought also limits restricts the movement of nutrients in the …oil water, reducing and decreases nutrient …heir availability to trees and consequently which would affect ... [2]

Deleted: lead to increased …levate surface temperatures and atmospheric CO_2 concentrations in the atmosphere… both of which change…ltering local and regional climate patterns and accelerate intensifying the frequency and intensity …everity of extreme events (Humphrey et al. 2018). These effects vary significantly responses …epending largely …n forest type and species composition, which combined… Together with the properties …haracteristics of the extreme events themselves (in terms of… such as their extent and severity- this variability) …omplicates our understanding of how drought influences …ffects the functionality of different forest ecosystems (Gharun et al. 2020; Shekhar et al. 2023a). These feedback loops underscore …ighlight the critical …rgent need to evaluate …ssess the repercussions of…ow climate extremes on …mpact different forest types, which play a pivotal role in…re crucial for sequestering significant portions of anthropogenic emissions from the atmosphere, under a drying climate… Our objectives in this …tudy are thus…ims to 1) quantify the extent and severity of the extreme conditions in 2022 – focusing on (in terms of …oil and atmospheric dryness-)…and compare that …hem to those of two past …revious extreme years (i.e., …003, 2018), 2) quantify the responses of different forest types to drought in terms of canopy browning and photosynthesis, and 3) relate connect the functional characteristics of the forests withto…the emerging responses observed at the canopy- … ... [3]

Deleted: (Longitude: 11°W - 32°E; Latitude: 35.8°N - 72°N, approximate area of 4.45 million km^2) gridded datasets of

Deleted: daily

Deleted: total precipitation (Precip; mm), …daily mean air temperature (Tair; °C), daily mean relative humidity (RH; %) and daily mean soil moisture (SM; m^3m^{-3}) for theof… ... [4]

longitudes from 11°W to 32°E, and latitudes from 35.8°N to 72°N, approximately 4.45 million km^2. We sourced the Tair and RH datasets from the E-OBS v27.0e dataset which provides daily data at 0.1°×0.1° spatial resolution (Cornes et al., 2018; Klein et al., 2002). We calculated daily mean vapor pressure deficit (VPD; kPa) from Tair and RH using Equation 1 (Dee et al. 2011).

$$VPD = (1 - \frac{RH}{100}) \times 0.6107 \times 10^{\frac{7.5 \times Tair}{237.3 + Tair}} \quad (1)$$

The SM dataset was extracted from the most recent reanalysis data from ECMWF's (European Centre for Medium-range Weather Forecasts) new land component of the fifth generation of European Reanalysis (ERA5-Land) dataset (daily at 0.1°×0.1° resolution; Munoz-Sabater et al., 2021). ERA5-Land provides soil moisture (SM) data at an hourly interval with a spatial resolution of 0.1° × 0.1°. For our analysis, we aggregated the hourly SM data into daily averages. Recent validation studies using in-situ measurements and satellite data have confirmed the high accuracy of surface SM simulations from ERA5-Land (Albergel et al., 2012; Lal et al., 2022; Muñoz-Sabater et al., 2021). Additionally, SM data from ERA5-Land have been utilized to investigate drought and global SM patterns (see Lal et al., 2023; Shekhar et al., 2024b). We re-sampled the Tair, VPD, and SM data from daily (0.1° × 0.1°) to 8-day (0.05° × 0.05°) intervals to align with the temporal and spatial resolution of the vegetation response dataset.

Forest canopy response dataset

In order to assess the forest canopy response to drought stress, we used two satellite-based proxies:

1) The structure-based NIRv (near-infrared of vegetation index derived from MODIS (Moderate Resolution Imaging Spectroradiometer; 8-day 500m x 500m MOD09Q1 v6.1 product) which is calculated using surface spectral reflectance at near-infrared band (RNIR) and red band (RRed) as shown in Equation 2 (Badgley et al. 2017). The calculated NIRv at 500m resolution was aggregated to a 0.05°×0.05° resolution (daily) by averaging.

Deleted: obtained
Deleted: Precip,
Formatted: Font: (Default) Arial
Formatted: Font: (Default) Arial
Deleted: (
Deleted: ;
Deleted: , and
Formatted: Font: (Default) Arial
Formatted: Font: (Default) Segoe UI Symbol
Formatted: Font: (Default) Arial
Formatted: Font: (Default) Arial
Formatted: Font: (Default) Arial
Formatted: Font: (Default) Arial
Formatted: Font: (Default) Arial
Deleted: The
Deleted: SM
Deleted: dataset
Deleted: was extracted from the most recent reanalysis data from ECMWF's (European Centre for Medium-range Weather Forecasts), new land component of the fifth generation of European Reanalysis (ERA5-Land) dataset (daily at 0.1°×0.1° resolution; Munoz-Sabater et al., 2021).
Deleted: ERA5-Land provides soil moisture (SM) data at an hourly interval with a spatial resolution of 0.1° × ... [5]
Formatted: Font: (Default) Arial
Formatted: Font: (Default) Arial
Formatted: Font: (Default) Arial
Deleted: ¶
Formatted: Font: (Default) Arial
Formatted: Font: (Default) Arial
Deleted: is
Deleted: demonstrated
Deleted: Furthermore
Deleted: s
Deleted: extensively used
Deleted: study
Deleted: We re-sampled (averaged) the Precip, Ta ... [6]
Deleted: t
Deleted: (
Deleted:),
Deleted: and
Deleted: (by mean) at

$$NIR_V = R_{NIR} \times \frac{R_{NIR} - R_{Red}}{R_{NIR} + R_{Red}} \quad (2)$$

2) The physiological-based reconstructed global OCO-2 (Observation Carbon Observatory - 2) solar induced fluorescence (GOSIF) dataset. Solar-induced fluorescence (SIF) is an energy flux (unit: $Wm^{-2}\mu m.sr^{-1}$) reemitted as fluorescence by the chlorophyll a molecules in the plants (Baker, 2008). Recent extensive research has established a strong link between Solar-Induced Fluorescence (SIF) and vegetation photosynthesis, validating SIF as an effective proxy for ecosystem gross primary productivity (GPP) (Li et al. 2018; Magney et al. 2019; Shekhar et al., 2022). The GOSIF dataset was created by training a Cubist Regression Tree model to gap-fill SIF retrievals from OCO-2 satellite. This was done using MODIS Enhanced Vegetation Index (EVI) and meteorological reanalysis data from MERRA-2 (Modern-Era Retrospective analysis for Research and Applications), which includes photosynthetically active radiation (PAR), VPD, and air temperature (see Li and Xiao, 2019). We downloaded GOSIF data set (v2) from the Global Ecology Data Repository (http://data.globalecology.unh.edu/data/GOSIF_v2/, last accessed on 25 July 2024). The GOSIF was available from 2000-2022 at 8-day temporal scale with a spatial resolution of 0.05°×0.05° (Li and Xiao, 2019).

GOSIF signals provide information about physiological response of forest photosynthesis while NIRv (a recently developed vegetation index) signals provide information about the health status of the canopy. NIRv is preferred over NDVI and EVI as it can isolate the vegetation signal, mitigate mixed-pixel issue, and partly address the influences of background brightness and soil contamination (Zhang et al. 2022). The two vegetation proxies used in this study are anticipated to offer complementary insights into vegetation response to drought.

Land cover dataset

In this study, we focused on five different types of forests (and woodlands) across Europe, namely, evergreen needleleaf forest (ENF), evergreen broadleaf forest (EBF), deciduous

Deleted: 2)
Deleted: T
Deleted: the physiological-based reconstructed global OCO-2 solar induced fluorescence (
Deleted: GO
Deleted: SIF)
Deleted: dataset
Deleted: . NIRv was estimated following Badgley et al. (2017) as:…
Deleted: NIRv was estimated following Badgley et … [7]
Deleted: ¶
Deleted: where, R_{NIR} and R_{Red} are the surface spec… [8]
Formatted: Superscript
Formatted: Superscript
Deleted: , and
Deleted: R
Deleted: recent extensive research
Deleted: haveis linked SIF to vegetation photosynth… [9]
Deleted: vapor pressure deficit (
Deleted:)
Deleted: access
Formatted: Font: (Default) Arial
Formatted: Font: (Default) Arial
Formatted: Font: (Default) Segoe UI Symbol
Formatted: Font: (Default) Arial
Formatted: Font: (Default) Arial
Formatted: Font: (Default) Arial
Deleted: ed
Formatted: Font: (Default) Arial
Deleted: indices
Deleted: expected
Deleted: provide
Deleted: information
Deleted: on
Formatted: Font: (Default) Arial
Formatted: Font: (Default) Arial
Formatted: Font: (Default) Arial
Formatted: Font: (Default) Arial
Formatted: Font: (Default) Arial
Formatted: Font: (Default) Arial
Deleted: function
Deleted: s

broadleaf forest (DBF), mixed forest (MF), and woody savannas (WSA). The spatial distribution of the five different forest types across Europe is shown in Figure 1. We used the yearly MODIS land cover product (MCD12C1 version 6.1 at 0.05°×0.05° resolution) for the years of 2001, 2006, 2011, 2016 and 2021, to extract total areas covered by each forest type. Area of each grid cell was calculated using trigonometric equations considering the latitudinal and longitudinal variations arising due to Earth's spherical shape (Ellipsoid). Only areas that were consistently identified as each forest type over the five-year period were included in the analysis. This means that only pixels common across these five years were selected, and with more than 50% of the 0.05°×0.05° pixel area identified as forests. The forested areas selected for this study encompassed 907,875 km², which represents approximately 24% of Europe's total land area. Out of the total area about 23% (206´212 km^2) was dominated by ENFs distributed largely across Northern Europe (NEU). Approximately 1% (7´000 km^2) of the area was dominated by EBFs, located entirely in Mediterranean Europe (MED), and about 10% (92´209 km^2) was dominated by DBF which was largely distributed across MED. Approximately 20% (174´934 km^2) of the total forested area was dominated by MFs largely dominating Central Europe (CEU), and about 47% (427´529 km^2) was dominated by WSA mostly found in NEU (Figure 1).

Formatted: Font: (Default) Arial

Formatted: Font: (Default) Segoe UI Symbol

Formatted: Font: (Default) Arial

Formatted: Font: (Default) Arial

Deleted: in those

Formatted: Font: (Default) Arial

Formatted: Font: (Default) Arial

Deleted:

Deleted: s

Deleted: the selected

Deleted: (Supplementary Fig. 1)

Formatted: Font: (Default) Arial

Formatted: Font: (Default) Arial

Formatted: Font: (Default) Arial

Formatted: Font: (Default) Segoe UI Symbol

Formatted: Font: (Default) Arial

Deleted:

Deleted: (Supplementary Fig. 1)

Formatted: Font: (Default) Arial

Deleted: The selected forested area in this study covered an area of 907´875 km^2 (about 24% of total land area of Europe)

Deleted: (Figure S1)

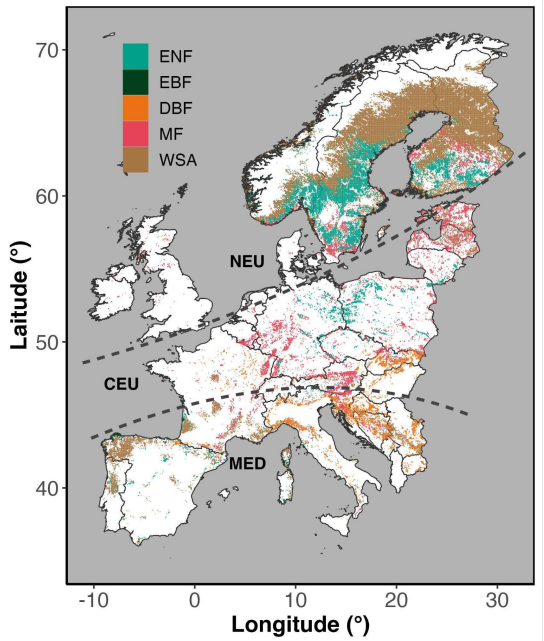

Figure 1 Spatial coverage of forests (ENF - evergreen needleleaf forest; EBF - evergreen broadleaf forest; DBF - deciduous broadleaf forest; MF - mixed forest), and woodlands (WSA - woody savannas) across Europe. Areas are differentiated into Northern Europe (NEU), Central Europe (CEU), and Mediterranean Europe (MED) following Markonis et al. (2021). The map is based on MODIS land cover product MCD12C1 (version 6.1).

Drought detection and statistical data analysis

The focus of our analysis was on the summer months during three extreme years of 2003, 2018 and 2022. For this purpose, we subset VPD, soil moisture (SM), and both vegetation proxies (NIRv and GOSIF) for the months of June, July, August (JJA) which consisted of fourteen 8-day periods, for each forested pixel between 2000 and 2022. We restricted our analysis to the months of June-July-August so our study is 1) comparable with existing studies focused on the summer drought 2) to capture the peak of the warm and dry conditions across Europe, that would be most stressful for the vegetation functioning, from the perspective of heat and water supply.

Formatted: Font: Not Bold

Deleted: , after selection (see methods)

Deleted: ¶

Deleted: ¶

Deleted: S

Formatted: Font: 12 pt, Not Bold, Italic

Formatted: Font: 12 pt, Not Bold, Italic

Deleted: our meteorological (Precip, Tair, and

Deleted:)

Deleted: y

Deleted: datasets

Deleted: comprised

Deleted: of

To account for the impact of the observed greening trend across Europe on vegetation proxy anomalies during the extreme years (2003, 2018, 2022), we applied a detrending process to the summer mean NIRv and GOSIF data. This detrending was performed pixel-wise from 2000 to 2022 using a simple linear regression model (Buras et al., 2020). We then calculated pixel-wise standardized summer anomalies, expressed as z-scores (Var_z), for all variables—VPD, SM, and the detrended NIRv and GOSIF (hereafter referred to as NIRv and GOSIF)—for each year, including the extreme years, using Equation 3.

$$Var_z\ (unitless) = \frac{Var - Var_{mean}}{Var_{sd}} \quad (3)$$

where, Var_{mean} and Var_{sd} are mean and standard deviation of any variable over the 2000-2022 period.

In drought identification studies, classification of 'normal' (not to be confused with normal distribution), 'drought' (used synonymously with 'dry'), or 'wet', is largely done using a standardized index, such as SPI (Standardized Precipitation Index), SPEI (Standardized Precipitation Evapotranspiration Index), and z-score among others (see Mishra and Singh, 2011). All studies that use a standardized index for classification, classify "normal" conditions when the index is between -1 and 1, and "below normal" conditions when the index is < -1, and "above normal" conditions when the index > 1 (Jain et al., 2015, Wable et al., 2019, Dogan et al., 2012, Tsakiris and Vangelis, 2004). In this study, we classified drought conditions as occurring when soil moisture is below normal (SMz < -1) and VPD is above normal (VPDz > 1), indicating both soil AND atmospheric dryness. This threshold-based approach using standardized anomalies aligns with established methods for drought identification and is pertinent for studying drought impacts on forests. Both soil moisture and VPD directly affect vegetation functioning, making them effective proxies for identifying environmental constraints on plant physiological performance. Furthermore, such classification of 'normal' (and thus, 'above normal' and 'below normal' used in this study) based on z-scores (also called standardized anomalies) can be done

Deleted: In order to exclude any
Deleted: the
Deleted: of vegetation proxies
Deleted: used detrended
Deleted: Detrending of summer mean NIRv and SIF from 2000-2022 was done pixel-wise based on a simple linear regression model
Formatted: Subscript
Deleted: We calculated pixel-wise standardized summer anomalies (in terms of z-score, Var_z) for all the variables (Var), i.e., Precip, Tair, VPD, SM, detrended NIRv, and detrended SIF (referred to NIRv and GOSIF from hereafter), for each extreme year (including extreme year) using Equation 3.
Deleted: ¶
Deleted: Z-scores less than -1 and more than 1 indicate significant negative and significant positive anomalies beyond normal variability. Var_z is calculated as:
Deleted: ¶
Deleted: Z
Deleted: y
Deleted: the
Deleted: i.e., presence of
Deleted: dryness
Deleted: approach
Deleted: (
Deleted:)
Deleted: methods
Deleted: in the literature and is relevant for studying drought impact on forests as we know from the body of literature that both SM and VPD directly influence vegetation functioning and thus are suitable proxies for identifying environmental limitations to plant physiological functioning

for any meteorological and/or response variables, such as NIRv and GOSIF done in this study, making the narration of results coherent across different variables.

We used the Pearson correlation coefficient (*r*) and partial correlation coefficients (Pr) to understand the spatial (across space for each year) and temporal (during each year) correlation of GOSIF and NIR_v anomalies with SM and VPD anomalies (Dang et al., 2022). We calculated the partial correlation coefficient using equations 4-7:

$$Pr(GOSIF,SM) = \frac{r(GOSIF,SM) - r(GOSIF,VPD)\times r(SM,VPD)}{\sqrt{1-r(GOSIF,VPD)^2} - \sqrt{1-r(SM,VPD)^2}} \quad (4)$$

$$Pr(GOSIF,VPD) = \frac{r(GOSIF,VPD) - r(GOSIF,SM)\times r(SM,VPD)}{\sqrt{1-r(GOSIF,SM)^2} - \sqrt{1-r(SM,VPD)^2}} \quad (5)$$

$$Pr(NIRv,SM) = \frac{r(NIRv,SM) - r(NIRv,VPD)\times r(SM,VPD)}{\sqrt{1-r(NIRv,VPD)^2} - \sqrt{1-r(SM,VPD)^2}} \quad (6)$$

$$Pr(NIRv,VPD) = \frac{r(NIRv,VPD) - r(NIRv,SM)\times r(SM,VPD)}{\sqrt{1-r(NIRv,SM)^2} - \sqrt{1-r(SM,VPD)^2}} \quad (7)$$

Results

Severity of the 2022 summer drought compared to 2018 and 2003

Figure 2 shows the extent and magnitude of anomalies (z-score) of VPD and top layer (0-7 cm) soil moisture content during the summer months in 2003, 2018, and 2022 across Europe. In summer 2022, particularly southern regions of Europe experienced the most pronounced increase in atmospheric (z-score > 1) and soil dryness (z-score < -1) (Figure 2) while in 2018 we observed the most widespread VPD and SM anomalies in northern Europe (Figure 2).

Deleted: (

Deleted:)

Deleted: Therefore, a

Deleted: Areas were categorized as under drought if $VPD_z > 1$ & $SM_z < -1$, and as normal areas if $-1 < VPD_z < 1$ & $-1 < SM_z < 1$.

Formatted: Border: Top: (No border), Bottom: (No border), Left: (No border), Right: (No border), Between : (No border)

Deleted: *SIF*

Deleted: the entire region of

Deleted: widespread drought

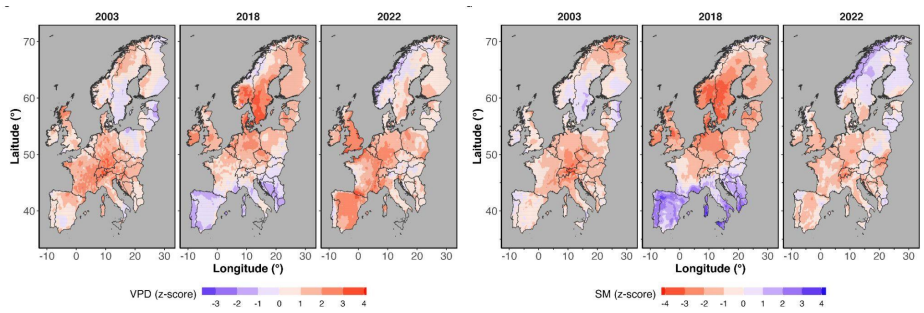

Figure 2 Standardized summer (JJA) anomalies (z-score) of mean vapor pressure deficit (VPD), and top layer (1-7 cm depth) soil moisture (SM) in 2003, 2018 and 2022, across the region of Europe.

Figure 3 shows the intensity of atmospheric and soil drought via z-score values of VPD and SM anomalies over the summer months (JJA) in 2003, 2018, and 2022. The total affected area displayed in Figure 3 is the sum of all pixels within the given z-score bin during the summer period where z-scores are averaged for each bin for the summer period. Restricted to forested areas, atmospheric and soil drought was 55% and 58% more extensive in 2018 compared to 2022, and in both years more extensive than in 2003 (Figure 3). In 2022, 28 Mha of forested areas in Europe experienced an extremely high VPD (z-score > 1), while in 2018, 63 Mha experienced such extreme conditions. In 2022, 21 Mha of forested areas experienced an extremely low soil moisture content (z-score < -1) while in 2018, 50 Mha of forests in Europe were affected by such extreme conditions. In 2003 an area of 25 Mha was affected by extremely dry air and a similar area was affected by extremely dry soil (Figure 3). A comparison of soil drought detected from SM at 0-100 cm showed a similar result in terms of area and magnitude of drought and thus we used SM at 0-7 cm soil layer for our analysis (see Supplementary Figure 1).

Formatted: Font: 12 pt

Deleted: (

Deleted: ,

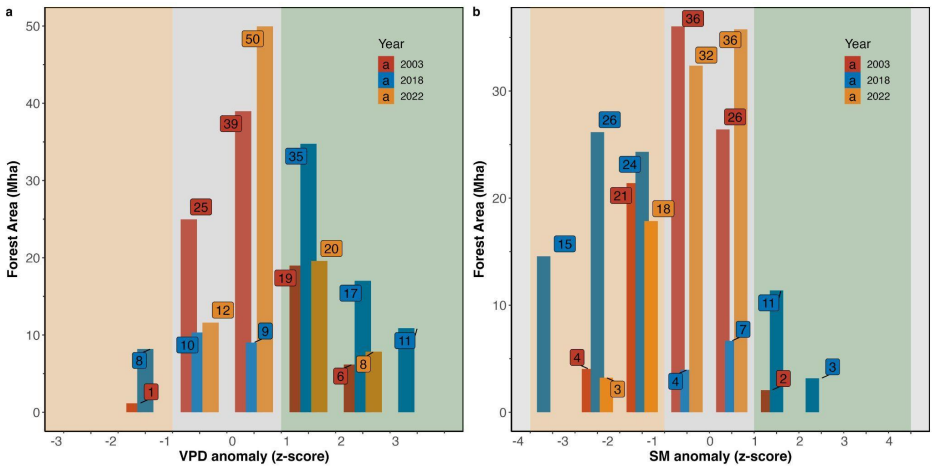

Figure 3 Intensity (z-score) and extent (area affected, Mha) of (a) VPD, and (b) SM anomalies across forested areas during the summer months (JJA). Z-score, values from -1 and 1 are considered normal (within 1 standard deviation of the mean). Orange-shaded area marks below normal and green-shaded area marks above normal conditions.

Forest canopy response to the 2022 drought

The intensity of GOSIF and NIRv anomalies over the summer months (JJA) in 2003, 2018, and 2022 are displayed in Figure 4. The extent shown in Figure 4 is the sum of all pixels within the given z-score bin during the summer period (z-scores are averaged for each bin). Compared to 2018, the extremely dry conditions in 2022 led to 30% increase in forested areas that exhibited declined photosynthesis (17 Mha in 2022 compared to 12 Mha in 2018) (Figure 4). The extent of the canopy browning observed in 2022 was similar to 2018, which in both years was 120% of the extent of observed canopy browning in 2003 (11 Mha compared to 5 Mha observed in 2003) (Figure 4).

Formatted: Font: 12 pt
Formatted: Font: 12 pt
Formatted: Font: 12 pt
Formatted: Font: 12 pt
Formatted: Font: 12 pt
Formatted: Font: Not Italic

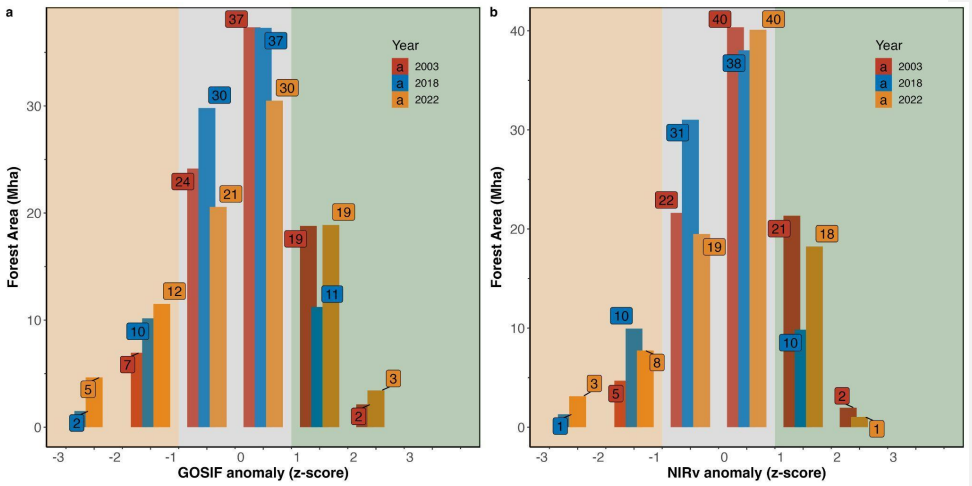

Figure 4 Intensity (z-score) and extent (area affected, Mha) for (a) GOSIF, and (b) NIRv anomalies across forested areas during the summer months (JJA). Z-score, values from -1 and 1 are considered normal (within 1 standard deviation of the mean). Orange-shaded area marks below normal and green-shaded area marks above normal conditions.

Figure 5a shows the GOSIF anomalies (z-score) across all forested areas in Europe. The intensity and extent of the GOSIF anomalies during the summer months (JJA) in each year are shown for different forest types in Figure 5b. Across specific forest types, DBFs showed the largest negative GOSIF anomaly in 2022 but the ENFs showed a positive GOSIF anomaly in 2022, both in terms of magnitude and in terms of the spatial extent of negative GOSIF anomalies (Figure 5).

Figure 6a shows the anomalies of NIRv (average z-score over the summer months) across all forested areas in Europe. The intensity and extent of the NIRv anomalies during the summer months (JJA) in each year are shown for different forest types in Figure 6b. In terms of canopy browning response (NIRv anomalies), the largest negative NIRv anomalies in 2022 were observed in southern Europe (Figure 6). Largest negative NIRv anomalies (indicated by the maximum anomaly) were observed in the DBFs in 2022,

Formatted: Font: 12 pt
Formatted: Font: 12 pt
Formatted: Font: 12 pt
Formatted: Font: 12 pt
Formatted: Font: 12 pt
Formatted: Font: 12 pt
Formatted: Font: 12 pt
Formatted: Font: 12 pt

fitting the declined GOSIF signals. The ENFs showed positive NIRv anomalies in 2022, in terms of magnitude, spatial coverage, and % of total area affected (Figure 6).

Deleted: however

Deleted: also both

Deleted: and

Deleted: in terms of the

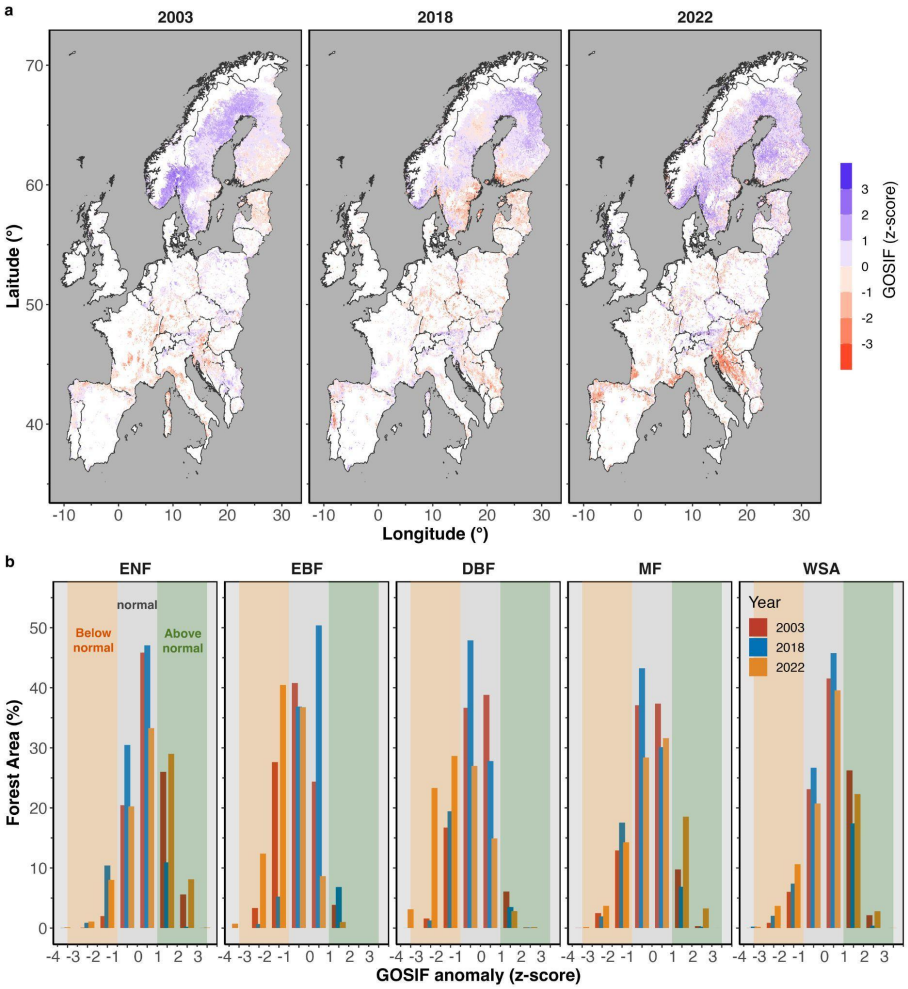

Figure 5 (a) GOSIF anomaly (in terms of z-score) across Europe, and (b) area coverage (in terms of percentage of total area for each forest type) during the summer months (JJA) in 2003, 2018 and 2022. Orange-shaded area marks below normal and green-shaded area marks above normal conditions. White areas on the map mark non-forested regions.

Formatted: Font: 12 pt
Formatted: Font: 12 pt
Formatted: Font: 12 pt
Deleted: in
Formatted: Font: 12 pt
Formatted: Font: 12 pt
Deleted:
Formatted: Font: 12 pt
Formatted: Font: 12 pt
Formatted: Font: 12 pt

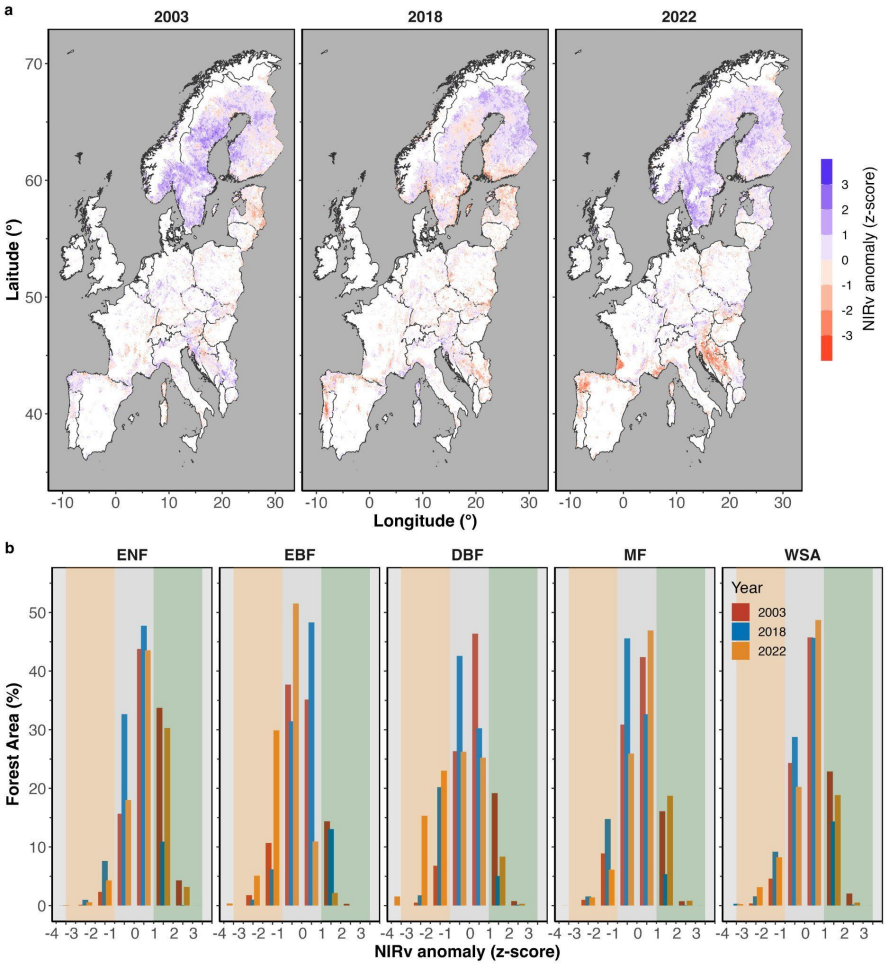

Figure 6 (a) NIRv anomaly (in terms of z-score) across Europe, and (b) area coverage (in terms of percentage of total area for each forest type) during the summer months (JJA) in 2003, 2018 and 2022. In panel (b) Orange-shaded area marks below normal and green-shaded area marks above normal conditions. White areas on the map mark non-forested regions.

Relationship between GOSIF and NIRv

Formatted: Font: Bold

Formatted: Normal

Deleted: ¶

Formatted: Space Before: 0 pt

In general, the values of NIRv and GOSIF were highly correlated (Supplementary Figure 2). The anomalies of NIRv and GOSIF were most correlated across WSAs (r^2 = 0.73 in 2018) and least correlated across the ENFs (Supplementary Figure 2). Figure 7 shows the spatial regression between standardized GOSIF anomalies with (a) VPD and (b) SM and Figure 8 shows the spatial regression between standardized NIRv anomalies with (a) VPD and (b) SM over the drought areas in summers 2003, 2018 and 2022. With the increase in VPD (i.e., increased atmospheric dryness), GOSIF values declined across all forest types, across all years, except in 2022 in the WSA, and in 2018 and 2022 in EBFs (Figure 7). With decrease in soil moisture (i.e., increased soil dryness), GOSIF values also declined overall (r^2 = 0.34), but not as strongly as with the increase in air dryness (r^2 = 0.39) (Figure 7). Across different forest types, GOSIF responded most strongly to VPD anomalies in the MFs (mean r^2 = 0.48), and responded most directly to changes in the soil moisture in the WSA (Figure 7).

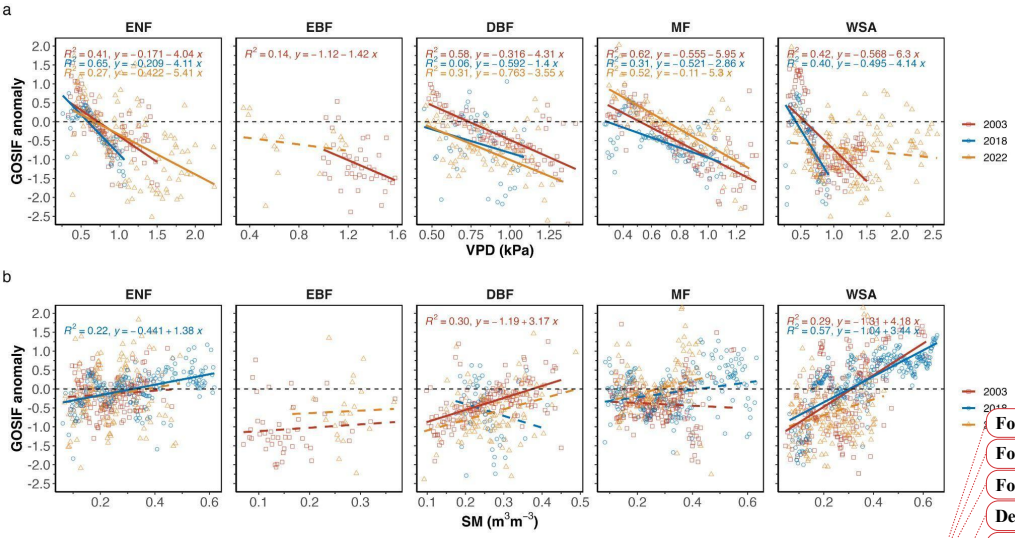

Figure 7 Spatial regression between standardized GOSIF anomalies with (a) VPD and (b) SM over the drought areas during the summer months (JJA) 2003, 2018 and 2022. Dashed lines mark an insignificant relationship (p > 0.05).

Deleted: 1
Deleted: in
Deleted: mean
Deleted:
Deleted: *r*
Deleted: 62
Deleted: 1
Deleted: positive anomalies
Formatted: Font: 12 pt
Formatted: Font: 12 pt
Formatted: Font: 12 pt
Deleted: in
Deleted: s
Formatted: Font: 12 pt
Formatted: Font: 12 pt
Formatted: Font: 12 pt
Formatted: Font: 12 pt
Formatted: Font: 12 pt

Between VPD and SM, in general GOSIF anomalies were more correlated with VPD than with SM anomalies, and the decline in VPD correlated well with the larger GOSIF decline that we observed in DBFs in 2022 and in ENFs in 2003 (Figure 7). Under typical conditions (regardless of drought), GOSIF's response to both air dryness and soil moisture anomalies was more pronounced than the response of NIRv (r^2 = 0.39 with GOSIF, compared to r^2 = 0.29 for NIRv) (Figure 7, 8).

Figure 9 shows the partial correlation coefficient between GOSIF with SM and VPD during summer months (JJA) for areas identified as affected (Figure 9a) and not affected (Figure 9b) by drought. The SM and VPD values across all forest types correlated well, but across DBFs the dryness in the atmosphere and the dryness in the soil were most correlated (Figure 9). Regarding canopy response to VPD, European Needleleaf Forests (ENF) exhibited the strongest reaction to changes in atmospheric dryness (Figure 9).

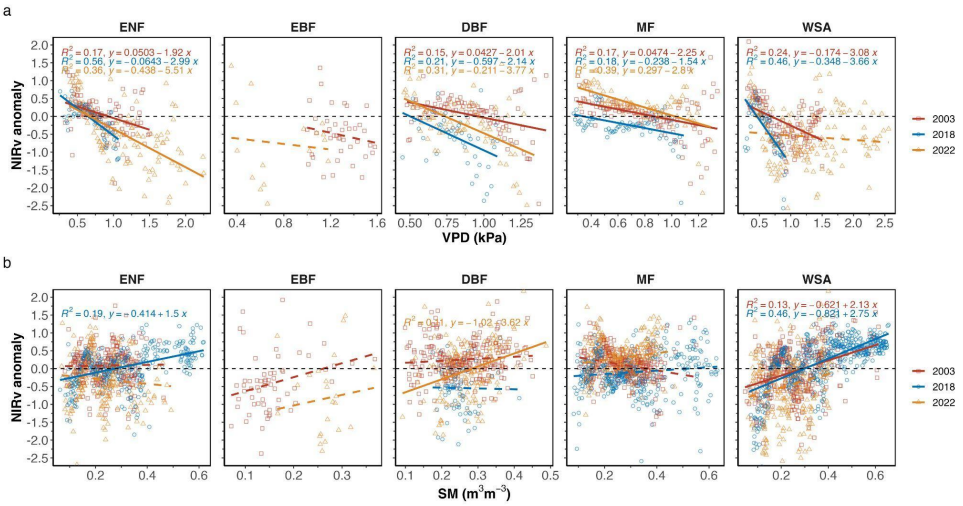

Figure 8. Spatial (over all pixels) regression between standardized NIRv anomalies with (a) VPD and (b) SM over the drought areas and normal areas in 2003, 2018 and 2022 during the summer months (JJA).

Deleted: Under general conditions (regardless of drought), response of SIF to both air dryness and soil moisture anomalies were larger than the response of NIRv…

Deleted: anomalies

Deleted: In terms of canopy response to VPD, ENF were the forests that responded most strongly to changes in the atmospheric dryness (Figure 9). ¶

Formatted: Font: 12 pt

Formatted: Font: 12 pt

Formatted: Font: 12 pt

Formatted: Font: 12 pt

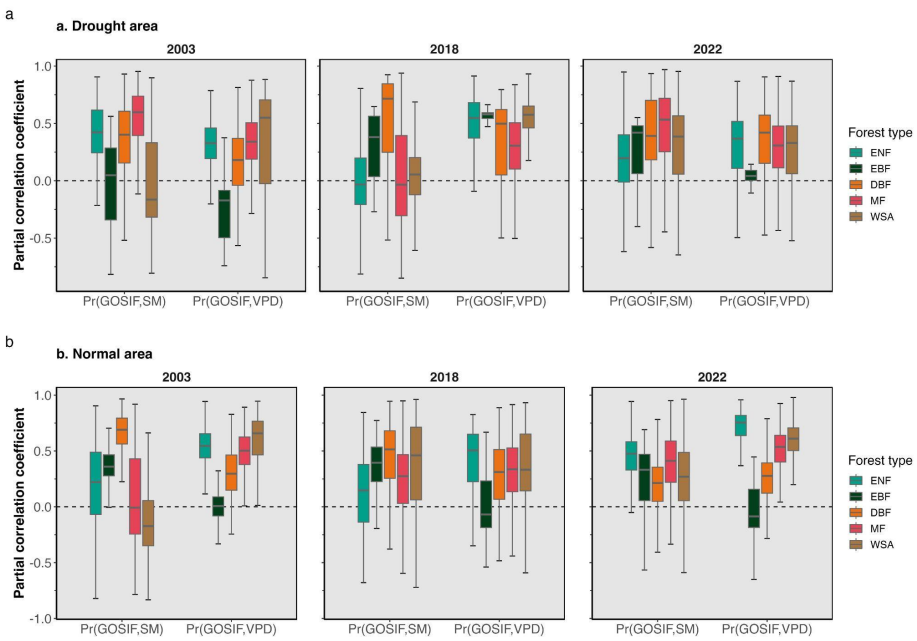

Figure 9. Temporal partial correlation coefficient of GOSIF with the absolute values of SM and VPD during the summer months (JJA) in 2003,2018 and 2022, for detected (a) drought areas and (b) normal areas. A comparable figure for NIRv can be found in Supplementary Figure 3.

Discussion

Severity of the 2022 summer drought

Although the years 2003, 2018, and 2022 are all categorized as "extreme," the specific characteristics of the extreme conditions varied significantly among these years. For example in 2003, widespread negative anomalies in soil moisture signaled a significant soil drought, whereas in 2022, widespread positive VPD anomalies indicated a notably drier atmosphere (Figure 3). It is important to note that ERA-5 Land datasets have been shown to underestimate the extent of European heatwaves in 2003, 2010, and 2018 (Duveiller et al., 2023), partly due to the use of a static leaf area index in their modeling

Formatted: Font: 12 pt
Formatted: Font: 12 pt
Formatted: Font: 12 pt
Formatted: Font: 12 pt
Formatted: Font: 12 pt
Formatted: Font: 12 pt
Formatted: Font: 12 pt
Formatted: Font: 12 pt
Formatted: Font: 12 pt
Deleted: similar
Deleted: is
Formatted: Font: 12 pt
Deleted: 2
Deleted: While the three selected years (2003, 2018, 2022) are all characterized as “extreme” years, characteristics of the extreme conditions varied largely across the years. …In 2003 f
In 2003 f
Deleted: In 2003 f
Deleted: the
Deleted: indicated
Deleted: while
Deleted: larger
Deleted: , signaled a
Deleted: mention
Deleted: European heatwaves
Deleted: incorporation of non-dynamic

framework. Consequently, the SM droughts in the years 2003, 2018, and 2022 may be more severe than indicated by our study, suggesting that our results might be somewhat conservative. The extensive summer drought in 2022 primarily impacted southern Europe, in contrast to the 2003 summer drought, which affected central Europe, and the 2018 drought, which extended to central and northern Europe (Figure 2) (Bastos et al., 2020). Consequently, the severe dry conditions in 2022 resulted in an average decline in GOSIF across forests that was 30% more widespread compared to 2018, and 60% more widespread compared to 2003 (Figure 4).These above-normal dry conditions during the summer reduced the photosynthetic capacity of plants and, consequently, the ecosystem's ability to absorb carbon from the atmosphere (Peters et al., 2018; van der Woude et al., 2023). Although the atmospheric and soil droughts in 2018 were more extensive and severe compared to 2022 (as indicated by the maximum observed z-scores), the adverse impact on forests, as reflected by the decline in GOSIF, was greater in 2022.

Canopy response to soil versus atmospheric dryness

The GOSIF dataset used in this study has been shown to be a reliable proxy for vegetation gross productivity, as demonstrated by comparisons with ground-based flux measurements (Shekhar et al. 2022; Pickering et al. 2022). It is important to note that GOSIF estimates are derived from a machine learning model trained with OCO-2 SIF observations, MODIS EVI data, and meteorological reanalysis data. As a result, the meteorological data used in our analyses are not entirely independent of the SIF data. However, this overlap is unlikely to impact our findings. A recent study that compared GOSIF with original OCO-2 data to assess the impacts of the 2018 U.S. drought found similar responses to drought between the two datasets (Li et al., 2020).
NIRv and SIF signals are well-correlated and effectively capture seasonal patterns in GPP (Getachew Mengistu et al. 2021). Although the strength of their relationship can vary with time, location, and forest type (see Supplementary Figure 2), reductions in SIF signals are directly associated with decreased photosynthesis. While both SIF and NIRv are reliable indicators of canopy responses to extreme climate events, SIF is more responsive to short-term climatic changes (Figure 7).

Deleted: Thus
Deleted: drought
Deleted: of
Deleted: ight
Deleted: larger
Deleted: shown in this
Deleted: thus making
Deleted: rather
Deleted: The widespread summer drought in 2022 affected mainly regions of southern Europe, as opposed to the 2003 summer drought that affected central Europe, or the 2018 summer drought that affected central and northern Europe (Figure 2) (Bastos et al. 2020). As a result, the extremely dry conditions in 2022 led to an average 30% more widespread decline in SIF across forests, compared to 2018, and a 60% more widespread decline compared to 2003 (Figure 4). ¶
Deleted: The above-normal drier conditions during the summer compromised the photosynthetic capacity of plants, and with that the capacity of the ecosyster ... [10]
Formatted: Space Before: 12 pt
Deleted: SIF
Deleted: , i.e., GOSIF
Deleted: products
Deleted: proven
Deleted: prove
Deleted: d
Deleted: show
Deleted: It should be noted that the GOSIF data a ... [11]
Deleted: correspond well
Deleted: are known to present
Deleted: well
Deleted: While the
Deleted: varies across time and space
Deleted: with changes in the
Deleted: 1
Deleted: can be
Deleted: linked to
Deleted: reduced
Deleted: good
Deleted: flects
Deleted: a better effect of
Deleted: changes in the
Deleted: e

Our analysis showed that across different regions, GOSIF anomalies corresponded more strongly to increased atmospheric dryness than to increased soil dryness (Figure 7). This supports the understanding that vapor pressure deficit plays a larger role in controlling SIF signals for trees over shorter time scales than soil moisture (Pickering et al. 2022). Over shorter time frames, trees can often mitigate soil moisture deficits through mechanisms within the rooting zone and by accessing deeper water sources, whereas there is no such buffer for the impact of atmospheric dryness on tree canopies. Ground-based observations in forest ecosystems, including both ecosystem and tree-level measurements, have shown that atmospheric dryness can constraint canopy gas exchange, even when soil moisture is not limiting (Gharun et al. 2014, Fu et al. 2022, Shekhar et al. 2024a). These findings highlight the importance of considering atmospheric dryness as a limiting factor for tree photosynthesis during extremely dry conditions and demonstrate the rapid response of various canopy types to increased levels of environmental dryness.

Canopy response to drought across different forest types

The spread of drought, measured as the total area across z-scores, exhibited distinct patterns in different years, leading to varied responses of different forest types to the climatic anomalies. Impact of drought on forests can significantly differ depending on the forest type, tree species, species composition, and past exposure to extreme conditions (Arthur and Dech 2016; Chen et al. 2022). Our analysis showed that conditions in summer 2022 reduced vegetation functioning across DBFs the most, as it was indicated by declined GOSIF signals (Figure 5). While deciduous broad-leaved forests were most negatively affected by the extreme conditions in 2022, Evergreen Needle-Leaf Forests (ENF) distributed in northern regions of Europe were not exposed to extremely dry conditions in 2022 and even showed enhanced canopy greening and GOSIF signals, through benefiting from the episodic warming (Forzieri et al. 2022). Under similar drought conditions, the mechanisms to cope with the level of drought stress vary largely among forest types, and depend on a combination of characteristics that control water loss through the coordination of stomatal regulation, hydraulic architecture, and root characteristics (e.g., rooting depth, root distribution, root morphology) (Gharun et al. 2020;

Deleted: fits the notion
Deleted: for trees,
Deleted: the
Deleted: over shorter time scales
Deleted: can be mitigated by various
Deleted: through plant´s access to
Deleted: sources of
Deleted: , whereas
Deleted: no such buffer exists
Deleted: s
Deleted: (e.g., based on
Deleted: or
Deleted:)
Deleted: impose
Deleted: s on
Deleted: within a
Deleted: range
Deleted: emphasize the significance
Deleted: in
Deleted: ,
Deleted: fast
Deleted: a range of
Deleted: sum of
Deleted: s
Deleted: different
Deleted: vary largely
Deleted: and factors that are controlled by

Deleted: distributed in northern regions of Europe showed enhanced canopy greening and
Deleted: GO
Deleted: SIF signals, through benefiting from the episodic warming (Forzieri et al. 2022). The mechanisms to cope with the level of drought stress, vary largely among forest types
Formatted: Font: 16 pt
Deleted: perth

Peters et al. 2023). Stomata of trees exhibit a high sensitivity to VPD fluctuations, causing a reduction in stomatal conductance as VPD increases, which, in turn, limits the exchange of CO_2 with the atmosphere during photosynthesis (Bonal and Guehl in 2011; Li et al. 2023). Different tree species show varying degrees of sensitivity in their stomatal responses to atmospheric dryness (Oren et al., 1999). For example, ring-porous species tend to maintain robust gas exchange under dry conditions, while diffuse-porous species, like those in ENFs, exhibit stronger stomatal regulation, reducing stomatal conductance as water availability decreases (Klein, 2014). This variability places plants on a spectrum of drought tolerance, reflecting their specific water relations strategies and leading to different responses among forests in similar climatic regions.

Increased frequency of extremes and declined resilience of forests

The increased canopy damage observed in 2022, despite less severe conditions compared to the previous extreme year, suggests a lasting impact on forest canopies that could lead to a decline in forest resilience in the face of more frequent drought events (Forzieri et al., 2022). A potential decline in the resilience of forests has significant implications for vital ecosystem services, including the forest's capacity to mitigate climate change. Consequently, there is an urgent need to consider these trends when formulating robust forest-based mitigation strategies. This need is especially critical given future projections indicating that the frequency and intensity of extreme dryness across Europe will more than triple by the end of the 21st century (Shekhar et al., 2024b). In this context, it is increasingly important to investigate the vulnerability of forests to external perturbations and to develop mitigation strategies tailored to site-specific ecophysiological and environmental factors that influence forest resilience to drought. Effective management strategies should be based on an understanding of these factors to mitigate the legacy effects of drought (McDowell et al., 2020; Wang et al., 2023; Shekhar et al., 2024a).

Conclusion

The severity of the 2022 summer drought, marked by increased atmospheric dryness, significantly compromised the photosynthetic capacity of trees, leading to widespread declines in vegetation functioning, especially in deciduous broad-leaved forests. Our

Deleted:

Deleted: Tree species exhibit varying degrees of sensitivity in their stomatal regulation response to increasing atmospheric dryness (Oren et al. 1999). For instance, ring-porous species tend to maintain robust gas exchange even under dry conditions, in contrast to diffuse-porous species like evergreen needle-leaf forests (ENFs), which adopt a stronger stomatal regulation, reducing stomatal conductance as water availability becomes more limited (Klein 2014). This variance places plants on a spectrum of drought tolerance (Klein 2014), representing their specific water relations strategy and leads to different responses of forests within similar climate regions.

Formatted: Space Before: 10 pt, Don't add space between paragraphs of the same style

Deleted: Higher degree of canopy damage that we observed in 2022, despite less severe conditions compared to the previous extreme year, points towards a lasting impact on forest canopies—a sign of decreased forest resilience in the face of more frequent drought events (Forzieri et al. 2022). The observed decline in forest resilience indicates possible significant implications for vital ecosystem services, including forest capacity for mitigating climate change. Consequently, there is an increasing urgency to consider these trends when formulating robust forest-based mitigation strategies. This is particularly critical as future projections indicate that the frequency and intensity of extreme dryness will continue to increase across Europe by more than 3-fold by the end of the 21st century (Shekhar et al. 2023b). In this context, it becomes increasingly important to investigate the vulnerability of forests to external perturbations, and to base the mitigation of drought legacy effects on management strategies that are tailored to site-specific ecophysiological and environmental factors that control the resilience of forests to drought (McDowell et al. 2020; Wang et al. 2023; Shekhar et al. 2024). ¶

findings underscore the importance of considering atmospheric dryness as a critical factor influencing canopy responses during extreme climatic events, alongside soil moisture deficits. Despite less severe overall conditions compared to previous extreme years, the greater canopy damage observed in 2022 suggests a growing vulnerability of forests to drought. This raises concerns about the future climate mitigation capacity of forest ecosystems, particularly as projections indicate a continued increase in the frequency and intensity of extreme dryness across Europe.

Deleted: The severity of the 2022 summer drought, characterized by increased atmospheric dryness, significantly compromised the photosynthetic capacity of trees, leading to widespread declines in vegetation functioning, particularly evident in deciduous broad-leaved forests. Our findings highlight the importance of considering atmospheric dryness as a critical factor influencing canopy responses during extreme climatic events, alongside soil moisture deficit. Despite less severe overall conditions compared to previous extreme years, the observed higher degree of canopy damage in 2022 suggests a declining resilience of forests to drought, raising concerns about the future climate mitigation capacity of forest ecosystems, as projections indicate a continued increase in the frequency and intensity of extreme dryness across Europe.¶

Competing interests

Mana Gharun is a guest editor of the Special Issue and the authors also have no other competing interests to declare

Acknowledgements

AS acknowledges funding from the SNF funded project EcoDrive (IZCOZ0_198094).

References

Albergel, C., De Rosnay, P., Balsamo, G., Isaksen, L., Munoz-Sabater, J., 2012. Soil moisture analyses at ECMWF: evaluation using global ground-based in situ observations. J. Hydrometeorol. 13, 1442–1460. https://doi.org/10.1175/JHM-D11-0107.1.

Anjileli, H., Huning, L.S., Moftakhari, H. et al. (2021) Extreme heat events heighten soil respiration. Sci Rep 11, 6632. https://doi.org/10.1038/s41598-021-85764-8

Arthur CM, Dech JP (2016) Species composition determines resistance to drought in dry forests of the Great Lakes - St. Lawrence forest region of central Ontario. Journal of Vegetation Science 27, 914-925.

Badgley G et al. (2017) Canopy near-infrared reflectance and terrestrial photosynthesis.Sci. Adv.3,e1602244.DOI:10.1126/sciadv.1602244

Bastos A et al. (2020) Impacts of extreme summers on European ecosystems: a comparative analysis of 2003, 2010 and 2018. Phil. Trans. R. Soc. B 375: 20190507. http://dx.doi.org/10.1098/rstb.2019.0507

Bauke, S. L., Amelung, W., Bol, R., Brandt, L., Brüggemann, N., Kandeler, E., Meyer, N., Or, D., Schnepf, A., Schloter, M., Schulz, S., Siebers, N., von Sperber, C., & Vereecken, H. (2022). Soil water status shapes nutrient cycling in agroecosystems from micrometer to landscape scales. Journal of Plant Nutrition and Soil Science, 185, 773–792. https://doi.org/10.1002/jpln.202200357

Bonal, D. & Guehl, J.-M. (2011) Contrasting patterns of leaf water potential and gas exchange responses to drought in seedlings of tropical rainforest species. Functional Ecology, 15, 490–496.

Buras, A., Rammig, A., and Zang, C. S. (2020) Quantifying impacts of the 2018 drought on European ecosystems in comparison to 2003, Biogeosciences, 17, 1655–1672, https://doi.org/10.5194/bg-17-1655-2020.

Chen, Y., Vogel, A., Wagg, C. et al. (2022) Drought-exposure history increases complementarity between plant species in response to a subsequent drought. *Nat Commun* 13, 3217. https://doi.org/10.1038/s41467-022-30954-9

Choat, B., Brodribb, T.J., Brodersen, C.R. et al. (2018) Triggers of tree mortality under drought. Nature 558, 531–539. https://doi.org/10.1038/s41586-018-0240-x

Cornes, R. C., van der Schrier, G., van den Besselaar, E. J. M., & Jones, P. D. (2018). An Ensemble Version of the E-OBS Temperature and Precipitation Data Sets. Journal of Geophysical Research: Atmospheres, 123(17), 9391–9409. https://doi.org/10.1029/2017JD028200

Formatted: Font: 12 pt

Formatted: Font: Not Bold

Formatted: Font: Not Bold

Formatted: Font: Not Bold

Formatted: Font: Not Bold

Formatted: Font: Not Bold

Formatted: Font: Not Bold

Formatted: Font: Not Bold

Formatted: Indent: Left: 0,32 cm, Line spacing: Multiple 1,15 li

Dang, C., Shao, Z., Huang, X., Qian, J., Cheng, G., Ding, Q., & Fan, Y. (2022). Assessment of the importance of increasing temperature and decreasing soil moisture on global ecosystem productivity using solar-induced chlorophyll fluorescence. Global Change Biology, 28(6), 2066–2080. https://doi.org/10.1111/gcb.16043

Dee, D. P., Uppala, S. M., Simmons, A. J., Berrisford, P., Poli, P., Kobayashi, S., Andrae, U., Balmaseda, M. A., Balsamo, G., Bauer, P., Bechtold, P., Beljaars, A. C. M., van de Berg, L., Bidlot, J., Bormann, N., Delsol, C., Dragani, R., Fuentes, M., Geer, A. J., Haimberger, L., Healy, S. B., Hersbach, H., Hólm, E. V., Isaksen, L., Kållberg, P., Köhler, M., Matricardi, M., McNally, A. P., Monge-Sanz, B. M., Morcrette, J. J., Park, B. K., Peubey, C., de Rosnay, P., Tavolato, C., Thépaut, J. N., and Vitart, F.: The ERA-Interim reanalysis: configuration and performance of the data assimilation system, Quarterly Journal of the Royal Meteorological Society, 137, 121 553-597, 10.1002/qj.828, 2011.

Drake JE, Tjoelker MG, Vårhammar A, Medlyn BE, Reich PB, Leigh A, Pfautsch S, Blackman CJ, López R, Aspinwall MJ, Crous KY, Duursma RA, Kumarathunge D, De Kauwe MG, Jiang M, Nicotra AB, Tissue DT, Choat B, Atkin OK, Barton CVM (2018) Trees tolerate an extreme heatwave via sustained transpirational cooling and increased leaf thermal tolerance. Glob Change Biol. 24: 2390–2402. https://doi.org/10.1111/gcb.14037

Deleted: ¶

Formatted: Font: 11 pt

Formatted: Indent: Left: 0,32 cm, Line spacing: Multiple 1,15 li

Formatted: Font: 11 pt

Formatted: Font: 11 pt

Formatted: Font: 11 pt

Duveiller, G., Pickering, M., Muñoz-Sabater, J., Caporaso, L., Boussetta, S., Balsamo, G., and Cescatti, A.: Getting the leaves right matters for estimating temperature extremes, Geosci. Model Dev., 16, 7357–7373, https://doi.org/10.5194/gmd-16-7357-2023, 2023.

Forzieri, G., Dakos, V., McDowell, N.G. et al. (2022) Emerging signals of declining forest resilience under climate change. Nature 608, 534–539. https://doi.org/10.1038/s41586-022-04959-9

Fu, Z., Ciais, P., Prentice, I.C. et al. Atmospheric dryness reduces photosynthesis along a large range of soil water deficits. Nat Commun 13, 989 (2022). https://doi.org/10.1038/s41467-022-28652-7

Gessler, A., Bottero, A., Marshall, J. and Arend, M. (2020), The way back: recovery of trees from drought and its implication for acclimation. New Phytol, 228: 1704-1709. https://doi.org/10.1111/nph.16703

Getachew Mengistu, A., Mengistu Tsidu, G., Koren, G., Kooreman, M. L., Folkert Boersma, K., Tagesson, T., Ardö, J., Nouvellon, Y., & Peters, W. (2021). Sun-induced fluorescence and near-infrared reflectance of vegetation track the seasonal dynamics of gross primary production over Africa. Biogeosciences, 18(9), 2843-2857. https://doi.org/10.5194/bg-18-2843-2021

Gharun M., Vervoort R.W., Turnbull T.L., Adams M.A. (2014) A test of how coupling of vegetation to the atmosphere and climate spatial variation affects water yield modelling in mountainous catchments 514, pp. 202-213. https://doi.org/10.1016/j.jhydrol.2014.04.037

Gharun M., Hörtnagl L., Paul-Limoges E., Ghiasi S., Feigenwinter I., Burri S., Marquardt K., Etzold S., Zweifel R., Eugster W., Buchmann N (2020) Physiological response of Swiss ecosystems to 2018 drought across plant types and elevationPhil. Trans. R. Soc. B37520190521 20190521. http://doi.org/10.1098/rstb.2019.0521

Gourlez de la Motte L, Beauclaire Q, Heinesch B, Cuntz M, Foltýnová L, Šigut L, Kowalska N, Manca G, Ballarin IG, Vincke C, Roland M, Ibrom A, Lousteau D, Siebicke L, Neiryink J, Longdoz B. (2020) Non-stomatal processes reduce gross primary productivity in temperate forest ecosystems during severe edaphic drought. Philos Trans R Soc Lond B Biol Sci. 375(1810):20190527. doi: 10.1098/rstb.2019.0527.

Haesen, S., Lembrechts, J. J., De Frenne, P., Lenoir, J., Aalto, J., Ashcroft, M. B., Kopecký, M., Luoto, M., Maclean, I., Nijs, I., Niittynen, P., van den Hoogen, J., Arriga, N., Brůna, J., Buchmann, N., Čiliak, M., Collalti, A., De Lombaerde, E., Descombes, P. … Van Meerbeek, K. (2023). ForestClim—Bioclimatic variables for microclimate temperatures of European forests. Global Change Biology, 29, 2886–2892. https://doi.org/10.1111/gcb.16678

Humphrey V, Zscheischler J, Ciais P, Gudmundsson L, Sitch S, Seneviratne SI. (2018) Sensitivity of atmospheric CO2 growth rate to observed changes in terrestrial water storage. Nature, 560 (7720): 628 DOI: 10.1038/s41586-018-0424-4.

Formatted: Indent: Left: 0,32 cm, Line spacing: Multiple 1,15 li

Formatted: German

Klein Tank, A. M. G., Wijngaard, J. B., Können, G. P., Böhm, R., Demarée, G., Gocheva, A., Mileta, M., Pashiardis, S., Hejkrlik, L., Kern-Hansen, C., Heino, R., Bessemoulin, P., Müller-Westermeier, G., Tzanakou, M., Szalai, S., Pálsdóttir, T., Fitzgerald, D., Rubin, S., Capaldo, M., … Petrovic, P. (2002). Daily dataset of 20th-century surface air temperature and precipitation series for the European Climate Assessment. International Journal of Climatology, 22(12), 1441–1453. https://doi.org/10.1002/joc.773

Klein, T. (2014), The variability of stomatal sensitivity to leaf water potential across tree species indicates a continuum between isohydric and anisohydric behaviours. Funct Ecol, 28: 1313-1320. https://doi.org/10.1111/1365-2435.12289

Lal, P., Shekhar, A., Gharun, M., Das, N.N., 2023. Spatiotemporal evolution of global long-term patterns of soil moisture. Sci. Total Environ. 867, 161470 https://doi.org/10.1016/j.scitotenv.2023.161470.

Lal, P., Singh, G., Das, N.N., Colliander, A., Entekhabi, D., 2022. Assessment of ERA5-land volumetric soil water layer product using in situ and SMAP soil moisture observations. Geosci. Rem. Sens. Lett. IEEE 19, 1–5. https://doi.org/10.1109/LGRS.2022.3223985 Li X et al. (2018) Solar-induced chlorophyll fluorescence is strongly correlated with terrestrial photosynthesis for a wide variety of biomes: first global analysis based on OCO-2 and flux tower observations Glob. Change Biol. 24 3990–4008.

Deleted: https://doi.org/10.1111/1365-2435.12289
Formatted: Font: 11 pt
Formatted: Font: 11 pt
Formatted: Font: 11 pt
Formatted: Font: 11 pt
Formatted: Font: 11 pt
Formatted: Font: 11 pt, German
Formatted: Font: 11 pt, German
Formatted: Font: 11 pt, German
Formatted: Font: 11 pt
Formatted: Font: 11 pt
Formatted: Font: 11 pt
Formatted: Font: 11 pt
Formatted: Font: 11 pt
Formatted: Font: 11 pt
Formatted: Font: 11 pt
Deleted: ¶
Formatted: Font: 11 pt
Formatted: Indent: Left: 0,32 cm, Line spacing: Multiple 1,15 li
Formatted: Font: 11 pt

Li, X., Xiao, J. (2019) A global, 0.05-degree product of solar-induced chlorophyll fluorescence derived from OCO-2, MODIS, and reanalysis data. *Remote Sensing*, *11*, 517; doi:10.3390/rs11050517.

Li, F., Xiao, J., Chen, J., Ballantyne, A., Jin, K., Li, B., Abraha, M., John, R. (2023) Global water use efficiency saturation due to increased vapor pressure deficit. Science, 381, 672-677. DOI: 10.1126/science.adf5041.

Magney T S et al. (2019) Mechanistic evidence for tracking the seasonality of photosynthesis with solar-induced fluorescence Proc. Natl Acad. Sci. USA 116 11640–5.

Marchin, R. M., Backes, D., Ossola, A., Leishman, M. R., Tjoelker, M. G., & Ellsworth, D. S. (2022). Extreme heat increases stomatal conductance and drought-induced mortality risk in vulnerable plant species. *Global Change Biology*, 28, 1133–1146. https://doi.org/10.1111/gcb.15976

Markonis, Y., Kumar, R., Hanel, M., Rakovec, O., Máca, P., AghaKouchak, A., (2021). The rise of compound warm-season droughts in Europe. Science Advances 7. https://doi.org/10.1126/sciadv.abb9668

McDowell, N. G. et al. (2020) Pervasive shifts in forest dynamics in a changing world. Science 368, eaaz9463.

Müller, L. M., and M. Bahn (2022) Drought legacies and ecosystem responses to subsequent drought. Global Change Biology 28:5086–103. doi:10.1111/gcb.16270.

Muñoz-Sabater, J., Dutra, E., Agustí-Panareda, A., Albergel, C., Arduini, G., Balsamo, G., Boussetta, S., Choulga, M., Harrigan, S., Hersbach, H., Martens, B., Miralles, D. G., Piles, M., Rodríguez-Fernández, N. J., Zsoter, E., Buontempo, C., & Thépaut, J. N. (2021). ERA5-Land: A state-of-the-art global reanalysis dataset for land applications. Earth System Science Data, 13(9), 4349–4383. https://doi.org/10.5194/essd-13-4349-2021

Peters, W., van der Velde, I.R., van Schaik, E. et al. Increased water-use efficiency and reduced CO2 uptake by plants during droughts at a continental scale. Nature Geosci 11, 744–748 (2018). https://doi.org/10.1038/s41561-018-0212-7

Peters, R.L., Steppe, K., Pappas, C., Zweifel, R., Babst, F., Dietrich, L., von Arx, G., Poyatos, R., Fonti, M., Fonti, P., Grossiord, C., Gharun, M., Buchmann, N., Steger, D.N. and Kahmen, A. (2023), Daytime stomatal regulation in mature temperate trees prioritizes stem rehydration at night. New Phytol, 239: 533-546. https://doi.org/10.1111/nph.18964

Pickering, M., Cescatti, A., and Duveiller, G. (2022) Sun-induced fluorescence as a proxy for primary productivity across vegetation types and climates, Biogeosciences, 19, 4833–4864, https://doi.org/10.5194/bg-19-4833-2022.

Formatted: Indent: Left: 0,32 cm, First line: 0 cm, Line spacing: Multiple 1,15 li

Oren, R., Sperry, J.S., Katul, G.G., Pataki, D.E., Ewers, B.E., Phillips, N. and Schäfer, K.V.R. (1999), Survey and synthesis of intra- and interspecific variation in stomatal sensitivity to vapour pressure deficit. Plant, Cell & Environment, 22: 1515-1526. https://doi.org/10.1046/j.1365-3040.1999.00513.x

Röthlisberger, M., Papritz, L. (2023). Quantifying the physical processes leading to atmospheric hot extremes at a global scale. Nature Geosci. 16(3), 210-216. doi:10.1038/s41561-023-01126-1.

Seidl, R., Thom, D., Kautz, M. et al. Forest disturbances under climate change. Nature Clim Change 7, 395–402 (2017). https://doi.org/10.1038/nclimate3303

Seneviratne, S. I., Zhang, X., Adnan, M., Badi, W., Dereczynski, C., Di Luca, A., Ghosh, S., Iskandar, I., Kossin, J., Lewis, S., Otto, F., Pinto, I., Satoh, M., Vicente-Serrano, S. M., Wehner, M., and Zhou, B. (2021) Weather and Climate Extreme Events in a Changing Climate, in: Climate Change 2021: The Physical Science Basis. Contribution of Working Group I to the Sixth Assessment Report of the Intergovernmental Panel on Climate Change, edited by: Masson-Delmotte, V., Zhai, P., Pirani, A., Connors, S. L., Péan, C., Berger, S., Caud, N., Chen, Y., Goldfarb, L., Gomis, M. I., Huang, M., Leitzell, K., Lonnoy, E., Matthews, J. B. R., Maycock, T. K., Waterfield, T., Yelekçi, O., Yu, R., and Zhou, B., Cambridge University Press, Cambridge, United Kingdom and New York, NY, USA, 1513–1766, https://doi.org/10.1017/9781009157896.013.

Shekhar, A., Hörtnagl, L., Buchmann, N., & Gharun, M. (2023). Long-term changes in forest response to extreme atmospheric dryness. Global Change Biology, 29, 5379–5396. https://doi.org/10.1111/gcb.16846

Shekhar A, Hörtnagl L, Paul-Limoges E, Etzold S, Zweifel R, Buchmann N, Gharun M (2024a) Contrasting impact of extreme soil and atmospheric dryness on the functioning of trees and forests. Science of the Total Environment 916, 169931. https://doi.org/10.1016/j.scitotenv.2024.169931

Shekhar A, Humphrey V, Buchmann N, Gharun M (2024b). More than three-fold increase of extreme dryness across Europe by end of 21st century. https://doi.org/10.21203/rs.3.rs-3143908/v2 (under review in Weather and Climate Extremes)

Shekhar A, Buchmann N and Gharun M (2022) How well do recently reconstructed solar-induced fluorescence datasets model gross primary productivity? Remote Sens. Environ. 283, 113282

Tripathy, K. P., & Mishra, A. K. (2023) How unusual is the 2022 European compound drought and heatwave event? Geophysical Research Letters, 50, e2023GL105453. https://doi.org/10.1029/2023GL105453

Formatted: Indent: Left: 0,32 cm, Line spacing: Multiple 1,15 li

Deleted: a

Deleted: https://doi.org/10.1016/j.scitotenv.2024.169931

Formatted: Indent: Left: 0,32 cm, Line spacing: Multiple 1,15 li

Formatted: Font: Bold, No underline, Font colour: Auto

Formatted: Indent: Left: 0,32 cm, First line: 0 cm, Line spacing: Multiple 1,15 li

Deleted: Shekhar A, Humphrey V, Buchmann N, Gharun M (20

Deleted: 43b). More than three-fold increase of dryness across Europe by end of 21st century. https://doi.org/10.21203/rs.3.rs-3143908/v2 (under review in Weather and Climate Extr

Formatted: Indent: Left: 0,32 cm, Line spacing: Multiple 1,15 li

van der Woude, A.M., Peters, W., Joetzjer, E. *et al.* Temperature extremes of 2022 reduced carbon uptake by forests in Europe. *Nat Commun* 14, 6218 (2023). https://doi.org/10.1038/s41467-023-41851-0

van der Molen MK, Dolman AJ, Ciais P et al (2011) Drought and ecosystem carbon cycling. Agric for Meteorol. 151(7):765–773. https://doi.org/10.1016/j.agrformet.2011.01.018

Zhang J, Xiao J, Tong X, Zhang J, Meng P, Li J, Liu P, Yu P (2022) NIRv and SIF better estimate phenology than NDVI and EVI: Effects of spring and autumn phenology on ecosystem production of planted forests. Agricultural and Forest Meteorology 315, 108819

Zhou, S., Yu, B. and Zhang, Y. (2023). Global concurrent climate extremes exacerbated by anthropogenic climate change. Sci. Adv. 9(10), p.eabo1638. doi:10.1126/sciadv.abo1638.

Wang B, Chen T, Xu G, Wu G, Liu G (2023) Management can mitigate drought legacy effects on the growth of a moisture-sensitive conifer tree species. Forest Ecology and Management 544, 121196. https://doi.org/10.1016/j.foreco.2023.121196

Formatted: Indent: Left: 0,32 cm, First line: 0 cm, Line spacing: Multiple 1,15 li

Formatted: Indent: Left: 0,32 cm, Line spacing: Multiple 1,15 li

Page 2: [1] Deleted Mana Gharun 31/07/2024 16:31:00

Page 4: [2] Deleted Mana Gharun 31/07/2024 16:44:00

Page 4: [2] Deleted Mana Gharun 31/07/2024 16:44:00

Page 4: [2] Deleted Mana Gharun 31/07/2024 16:44:00

Page 4: [2] Deleted Mana Gharun 31/07/2024 16:44:00

Page 4: [2] Deleted Mana Gharun 31/07/2024 16:44:00

Page 4: [2] Deleted Mana Gharun 31/07/2024 16:44:00

Page 4: [2] Deleted Mana Gharun 31/07/2024 16:44:00

Page 4: [2] Deleted Mana Gharun 31/07/2024 16:44:00

Page 4: [2] Deleted Mana Gharun 31/07/2024 16:44:00

Page 4: [2] Deleted Mana Gharun 31/07/2024 16:44:00

Page 4: [3] Deleted Mana Gharun 31/07/2024 16:47:00

Page 4: [3] Deleted Mana Gharun 31/07/2024 16:47:00

Page 4: [3] Deleted Mana Gharun 31/07/2024 16:47:00

Page 4: [3] Deleted Mana Gharun 31/07/2024 16:47:00

Page 4: [3] Deleted **Mana Gharun** **31/07/2024 16:47:00**

Page 4: [3] Deleted **Mana Gharun** **31/07/2024 16:47:00**

Page 4: [3] Deleted **Mana Gharun** **31/07/2024 16:47:00**

Page 4: [3] Deleted **Mana Gharun** **31/07/2024 16:47:00**

Page 4: [3] Deleted **Mana Gharun** **31/07/2024 16:47:00**

Page 4: [3] Deleted **Mana Gharun** **31/07/2024 16:47:00**

Page 4: [3] Deleted **Mana Gharun** **31/07/2024 16:47:00**

Page 4: [3] Deleted **Mana Gharun** **31/07/2024 16:47:00**

Page 4: [3] Deleted **Mana Gharun** **31/07/2024 16:47:00**

Page 4: [3] Deleted **Mana Gharun** **31/07/2024 16:47:00**

Page 4: [3] Deleted **Mana Gharun** **31/07/2024 16:47:00**

Page 4: [3] Deleted **Mana Gharun** **31/07/2024 16:47:00**

Page 4: [3] Deleted **Mana Gharun** **31/07/2024 16:47:00**

Page 4: [3] Deleted **Mana Gharun** **31/07/2024 16:47:00**

Page 4: [3] Deleted Mana Gharun 31/07/2024 16:47:00

Page 4: [3] Deleted Mana Gharun 31/07/2024 16:47:00

Page 4: [3] Deleted Mana Gharun 31/07/2024 16:47:00

Page 4: [3] Deleted Mana Gharun 31/07/2024 16:47:00

Page 4: [3] Deleted Mana Gharun 31/07/2024 16:47:00

Page 4: [3] Deleted Mana Gharun 31/07/2024 16:47:00

Page 4: [3] Deleted Mana Gharun 31/07/2024 16:47:00

Page 4: [3] Deleted Mana Gharun 31/07/2024 16:47:00

Page 4: [3] Deleted Mana Gharun 31/07/2024 16:47:00

Page 4: [3] Deleted Mana Gharun 31/07/2024 16:47:00

Page 4: [3] Deleted Mana Gharun 31/07/2024 16:47:00

Page 4: [3] Deleted Mana Gharun 31/07/2024 16:47:00

Page 4: [4] Deleted Mana Gharun 05/06/2024 13:16:00

Page 4: [4] Deleted Mana Gharun 05/06/2024 13:16:00

Page 5: [5] Deleted Ankit Shekhar 25/07/2024 03:52:00

Page 5: [6] Deleted **Mana Gharun** **31/07/2024 17:13:00**

Page 6: [7] Deleted **Ankit Shekhar** **25/07/2024 04:56:00**

Page 6: [8] Deleted **Ankit Shekhar** **25/07/2024 04:56:00**

Page 6: [9] Deleted **Mana Gharun** **31/07/2024 17:19:00**

Page 20: [10] Deleted **Mana Gharun** **31/07/2024 17:53:00**

Page 20: [11] Deleted **Mana Gharun** **31/07/2024 17:55:00**